STATISTICS, OPTIMIZATION AND INFORMATION COMPUTING
Stat., Optim. Inf. Comput., Vol. **x**, Month 202x, pp 0–12.
Published online in International Academic Press (www.IAPress.org)

Environmental data modeling of different locations in Iraq based on the Ramos-Louzada distribution and its extensions

Rikan A. Ahmed [1], Zakariya Yahya Algamal [1,*], Zakariya Nafi Shehab [2]

[1]*Department of Statistics and Informatics, University of Mosul, Mosul, Iraq*
[2]*Department of Environmental Systems and Information, Environmental Researches Center, University of Mosul, 41002 Mosul, Nineveh, Iraq*

Abstract Environmental data modeling, particularly wind speed variations across Iraq's diverse regions, supports renewable energy assessment and climate risk management amid fossil fuel dependency challenges. This study applies the Ramos-Louzada (RL) distribution and its extensions Generalized RL (GRL), Inverse Power RL (IPRL), Exponentiated GRL (EGRL), Inverse RL (IRL), and Ramos-Louzada Exponential (RLE) distribution to hourly 2023 wind speed data from four Iraqi cities: Basrah, Al-Sulaymaniyah, Tikrit, and Al-Kut. Parameters are estimated via maximum likelihood, with model performance evaluated using several criteria. Results reveal location-specific fits, with average wind speeds ranging from 2.75 m/s (Al-Sulaymaniyah) to 4.76 m/s (Basrah), all positively skewed and moderately kurtosis. The IRL distribution outperforms others across all sites, achieving the highest coefficient of determination (R^2) (0.9758–0.9877) and the lowest root mean square error (0.0332–0.0432), Akaike information criterion, Bayesian information criterion, and the Kolmogorov–Smirnov statistic (KS), surpassing IPRL (second-best) and RL baselines. While, RLE distribution consistently ranks lowest. Further, IRL distribution also exceeds Weibull distribution benchmarks, with superior R^2 and reduced KS by up to 52%. These findings highlight RL extensions' flexibility for heavy-tailed, skewed wind regimes, informing wind energy potential, site-specific turbine design, and environmental forecasting in Iraq.

Keywords Ramos-Louzada distribution, wind speed modeling, environmental modeling, Kolmogorov–Smirnov test, renewable energy

DOI: 10.19139/soic-2310-5070-3580

1. Introduction

Energy and energy consumption has become an integral part of socio-economic development around the world and continues to rise at an alarming rate through social practices (as a result of technological advancement). Currently, most energy needs are provided for primarily by fossil fuels; however, this is not sustainable and will run out in the future. In addition, there is a widespread consensus that using fossil fuels has many negative effects on the global environment [1]. The overwhelming reliance on fossil fuels to support the rapid development of socioeconomic systems has resulted in many environmental issues, including climate change, the greenhouse effect, and an increasing lack of energy [2, 3]. Ultimately, this will put human health and the ecological balance at a high risk while jeopardizing the sustainable development of societies and economies throughout the world. As such, interest around the globe has grown rapidly in exploring and developing alternative energy sources that are not only environmentally friendly but also cleaner and more abundant in nature.

Renewable energy, sometimes referred to as clean energy, is a type of sustainable energy that is derived from unlimited nature-made sources or naturally occurring processes that constantly replenish themselves. In many

*Correspondence to: Zakariya Yahya Algamal (Email: zakariya.algamal@uomosul.edu.iq). Department of Statistics and Informatics, University of Mosul, Mosul, Iraq.

ISSN 2310-5070 (online) ISSN 2311-004X (print)

cases, the use of renewable energy will contribute to sustainable economic development by factoring environmental considerations into their development strategies [4]. Wind power is one of the fastest-growing renewable energy types worldwide. As an environmentally friendly energy source, wind energy offers many social, environmental and economic benefits. In addition, wind power is widely available, does not contribute to greenhouse gas emissions and does not deplete natural resources [5]. The worldwide acceptance of wind energy as a resource has grown as a result of the worldwide increase in the generation of electricity from wind use from 966 GW in 2023 to 906GW in 2022. The total amount of wind energy generated globally increased to 906 GW in 2022, which is almost double the amount generated in 2016 (approximately 90 percent, or 486 GW) [6]. A suitable distribution for simulation, forecasting, and risk management in the wind energy business improves the efficiency of designing and operating systems in a sustainable manner [7, 8, 9, 10, 11].

It is critical to conduct a comprehensive evaluation of wind energy resources to effectively and economically utilize wind power [12]. Two major components will play an important role when evaluating wind energy resources: the location where the wind farms will be located and the statistical distribution of wind speed characteristics [13]. An important aspect of this will allow researchers and engineers to determine the potential of wind energy and then develop an economically viable and technically sound design of a wind energy system based on that assessment [14]. The wind speed data is generally positive skewed, which means the majority of the data consists of winds having low to moderate speeds, with a few data points having high wind speeds. Wind speed data is generally characterized by heavy tails (e.g., occasional very high wind speeds), and are poorly fitted to a normal distribution model. Thus, utilizing different statistical distributions and models to model wind speed data and account for wind speed characteristics can provide an accurate representation.

The Weibull distribution function is widely used to evaluate and model wind speed data in many geographic areas because it provides an easy-to-use formulation and has a wide range of possible values [15]. As various studies have shown under the Weibull distribution, there are deficiencies in modelling the wind speed regimes; that is, both high or low wind speeds or even the presence of multimodal patterns of wind speed in nature [16-20]. One of the reasons for this is that the Weibull distribution only contains one shape parameter; therefore, when looking at other distributions containing a single shape parameter, the skewness and kurtosis measures range from being between 0- to 5.0. Consequently, this limits the ability of a distribution to represent actual data [2].

As such, various other distributions that are more versatile in modeling the wind speed data have been employed, and these include the Ramos-Louzada (RL) distribution. The distribution is especially appropriate to model wind data because it is flexible to describe heavy-tailed phenomena, skewness, and extreme values that are important in the analysis of wind speed. In most cases, wind speed observations tend to have extreme values, which could be misrepresented by normal forms of distribution such as Weibull. The CDF and PDF have a form that is capable of modeling data with skewness and that has a heavy right tail. The shape parameter of the RL distribution provides the flexibility to capture many types of skewness and kurtosis, and therefore, it is suitable in the case of wind speed data ,which often exhibit such properties [21].

The RL distribution has been discovered to be very effective with the modeling of wind speed data and has successfully captured the central tendency and properties of the tails. Such a model is better than the conventional distributions, including Weibull and log-normal distributions in cases when the data is very skewed and contains the characteristic of a heavy tail [22]. A number of extensions and generalizations have also been suggested to add more flexibility to the RL distribution.

These include the generalized Ramos-Louzada [23], inverse power Ramos–Louzada distribution [24], exponentiated generalized Ramos-Louzada distribution [25], inverse Ramos-Louzada distribution [26], Ramos Louzada exponential distribution [27], and the five-parameter Kumaraswamy Ramos-Louzada Weibull distribution [28]. Probably the most widely used methods to estimate the parameters of RL distribution, and models based on it, include Maximum Likelihood Estimation, Bayesian inference or the Method of Moments. It is therefore of utmost importance that these parameters be properly estimated so as to make credible predictions and estimates of the above models [29]. A number of research articles have also stated that RL distribution and variants could be superior to their classical equivalents in terms of goodness-of-fit and predictive validity of wind speed data. These distributions worked especially in areas that had high winds speed as the tail behavior was well captured in wind speed distribution [30, 43].

This paper will use the RL distribution and its derivatives to the hourly wind speed data of four key Iraqi cities (Al Sulaymaniyah, Tikrit, Al-Kut and Basrah) of the year 2023. It is intended to provide a proper modeling of the distribution of the different statistical characteristics present in the wind speed distributions, including heavy tails and skewness. The complex statistical models allow tracing the behavior of wind speed in more exact and detailed detail of different areas of Iraq, therefore making a significant contribution to valuable information in the meteorological evaluation, renewable energy utilization, and environmental management.

The Main contributions are:

1. Propose the use of the Ramos–Louzada (RL) distribution and five of its extensions for modeling hourly 2023 wind speed data in four key Iraqi cities (Basrah, Al-Sulaymaniyah, Tikrit, Al-Kut).
2. Estimate model parameters via maximum likelihood and systematically compare all RL-based models with each other and with the standard Weibull benchmark using several criteria.
3. Empirically show that the inverse Ramos–Louzada (IRL) distribution consistently provides the best fit at all locations, achieving the highest performance.
4. Demonstrate that IRL also outperforms the Weibull distribution, thereby establishing RL extensions as flexible and robust tools for positively skewed, heavy-tailed wind regimes in Iraq.
5. Provide location-specific insights into wind regimes (mean, variability, skewness, kurtosis) that can directly inform site selection, turbine design, and environmental and energy planning in Iraq.

2. Wind speed data

For this research project, we used 2023 hourly wind speed datasets created using the MERRA-2 Wind Speed at 10 Meter dataset, which represents wind speed as meters/second, for each of the four purposely sampled Iraqi cities: Al-Sulaymaniyah, Tikrit, Al-Kut and Basrah (shown in Figure 1). The MERRA-2 Wind Speed at 10 Meter data is produced by the Modern-Era Retrospective analysis for Research and Applications, Version 2. Each site has 8092 hourly observations covering nearly the entire year, allowing researchers to provide high quality hourly temporal data for a comprehensive wind speed variability analysis across diverse climates and geographic areas of Iraq.

The geography of Northern Iraq's Al-Sulaymaniyah region contributes to a very complex wind regime that varies in intensity based on elevation and a rugged terrain. The hourly recorded wind speeds in 2023 show substantial fluctuations of diurnal and seasonal winds and are likely the result of interactions between local geographic features and larger-scale weather phenomena. The research indicates a significant increase of wind speed during the winter months due to frontal systems, while in summer, wind pattern attributes almost entirely to the thermal contrasts between the surrounding plains and mountains. Al-Sulaymaniyah also has the lowest average wind speed and least variability. In addition, the skewness and kurtosis are both large positive numbers, indicating that the distribution of daily wind speeds is very long-tailed to the right (longer periods of low wind speeds with a small number of high wind speeds) and has a higher peak value compared to a normal Gaussian distribution.

Located in Iraq's semi-arid central area, Tikrit has a stable wind regime, as seen by hourly data compiled over the course of 2023. Compared to Al Sulaymaniyah, the diurnal cycle is less pronounced; however, average wind speeds remain moderate at best. In addition, spring and autumn have produced higher-gust winds caused by weather systems moving across the area. Therefore, Tikrit is an important location for understanding the feasibility of producing wind energy. Tikrit has been established as having moderate wind velocities relative to other urban centres. The measures of skewness and kurtosis also indicate positivity which means the distribution of wind data across the entire year is unevenly skewed to the right, along with slightly heavier tails than a normal distribution would produce.

Al-Kut, located in southern Iraq along the Tigris River, demonstrates the characteristics associated with flat lands close to the river. Al-Kut has high-frequency hourly observation data of wind speed available for 2023, indicating a fairly consistent moderation or slight variation from day to night during spring and summer; due primarily to the effect of both regional and local convection, as well as wind patterns resulting from the geographical positioning of the area. The data show wind speed measured in the hot months of the year at Al-Kut were consistent with other

locations measured for the same time frame; thus, wind potential as a source of energy generation can be accurately assessed. Al-Kut ranks second in terms of average hourly wind speed, as well as its variance. In addition, wind speed frequency distribution is highly positively skewed and very close to a mesokurtic (peaked) distribution.

As it is located in southern Iraq, Basrah has the highest wind speeds of the four cities discussed here. Wind speeds are primarily the result of its location near the Persian Gulf in addition to the influence of the "Shamal winds". Data from 2023 show strong daily patterns of wind speed. In the afternoon and early evening hours, average hourly wind speeds are at their highest levels, especially during the months in which Shamal winds are most prevalent. Other data indicate that throughout the late spring and early summer season, wind speeds in Basrah have been significantly greater than average, attributable to the increased wind speed associated with the Shamal's seasonal intensity. Due to this ongoing wind activity, Basrah is well-suited for a study on the wind energy potential of this region. Basrah continues to have the highest average wind speed and greatest range of variability of the four locations, indicating a tendency toward a high number of low speed wind events and very few occurrences of extreme wind (speed is measured at high values at random times). The influence of Iraq's wide variety of geographic features, such as coastlines, mountains and other arid desert regions, and how these different geographic characteristics contribute to the different types of wind patterns (Table 1).

Table 1. Descriptive of the locations

Location	Longitude	Latitude	Elevation (m)
Basrah	47° 46' 49.44" E	30° 30' 30.67" N	3.14
Al-Sulaymaniyah	45° 25' 58.44" E	35° 33' 53.86" N	1056.28
Tikrit	43° 40' 59.99" E	34° 35' 59.99" N	107.89
Al-Kut	45° 49' 5.41" E	32° 30' 46.08" N	18.23

3. RL distribution and its extensions

The wind speed is taken to be a random variable. Thus, the application of statistical distributions in the modeling of the wind speed is a widespread practice in areas of renewable energy, climate, and engineering [31, 44, 45, 46, 47]. A number of probability distributions have been applied to model the data of wind speed although with varying success rates depending on the site and the data particulars. Weibull distribution is the most utilized distribution [17, 32, 33, 34]. Nonetheless, Weibull distribution differs across locations. This makes it hard to combine the Weibull distribution to fit all the data of wind speed [5, 48, 49, 50, 51].

The RL distribution is a one-parameter continuous probability model introduced for lifetime data analysis [35, 36]. It offers an increasing concave hazard rate ideal for capturing skewed, heavy-tailed environmental phenomena such as pollutant lifetimes or drought durations [37]. The RL cumulative distribution function (CDF) and the probability density function (PDF) with scale parameter, γ of the wind speed, z, can be expressed, respectively, as

$$F_{\mathrm{RL}}(z;\gamma) = 1 - \frac{(\gamma + \gamma^{-1}z - 1)e^{-\frac{z}{\gamma}}}{(\gamma - 1)}, \quad z > 0,\ \gamma \geq 2 \tag{1}$$

$$f_{\mathrm{RL}}(z;\gamma) = \frac{(\gamma^2 - 2\gamma + z)e^{-\frac{z}{\gamma}}}{\gamma^2(\gamma - 1)}, \quad z > 0,\ \gamma \geq 2 \tag{2}$$

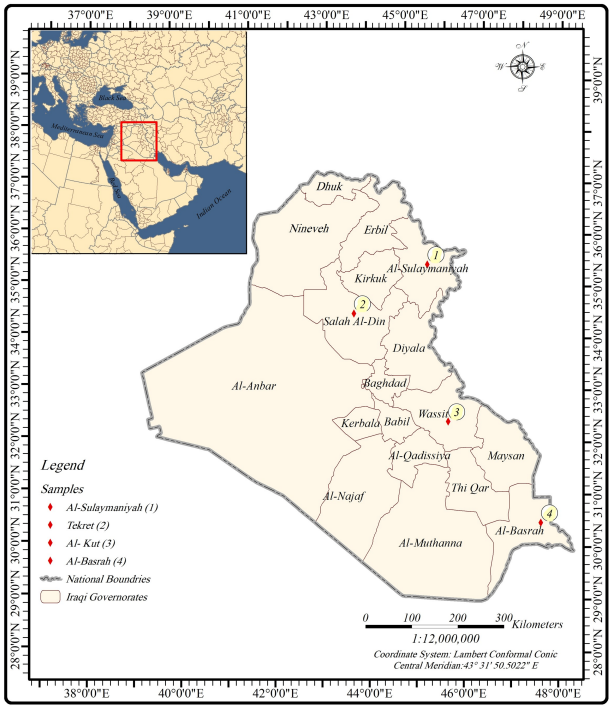

Figure 1. The selected locations of the wind speed data.

3.1. Generalized Ramos-Louzada (GRL) distribution

Al-Mofleh, Afify and Ibrahim [23] were the first to propose an extension of the RL distribution with a two-parameter named GRL distribution having the CDF and PDF as:

$$F_{\mathrm{GRL}}(z;\gamma,\beta) = 1 - \left(\frac{1}{\gamma-1}\right)\left(\gamma - 1 + \frac{z^{\beta}}{\gamma}\right) e^{-\frac{z^{\beta}}{\gamma}} \tag{3}$$

$$f_{\mathrm{GRL}}(z;\gamma,\beta) = \frac{\beta}{\gamma(\gamma-1)} z^{\beta-1}\left(\gamma + \frac{z^{\beta}}{\gamma} - 2\right) e^{-\frac{z^{\beta}}{\gamma}}, \quad z>0, \beta>0 \tag{4}$$

where $\beta > 0$ is the shape parameter.

4. Inverse power Ramos–Louzada (IPRL) distribution

The IPRL distribution is proposed an extension of the RL distribution by Al Mutairi, Hassan [24, 52, 53, 54]. It has two parameters and is obtained by an inverse-power transformation the random variable that has RL distribution, $w = 1/z^{\alpha}$. The IPRL CDF is expressed as

$$F_{\mathrm{IPRL}}(w;\gamma,\alpha) = \frac{(\gamma + \gamma^{-1}w^{-\alpha} - 1)e^{-\gamma^{-1}w^{-\alpha}}}{(\gamma-1)}, \quad w>0,\ \gamma \geq 2,\ \alpha>0 \tag{5}$$

and the corresponding PDF of IPRL is given as follows:

$$f_{\mathrm{IPRL}}(w;\gamma,\alpha) = \frac{[\alpha + \alpha(\gamma-2)\gamma w^{\alpha}]\, w^{-2\alpha-1} e^{-\gamma^{-1}w^{-\alpha}}}{\gamma^2(\gamma-1)}, \quad w>0,\ \gamma \geq 2,\ \alpha>0 \tag{6}$$

5. Exponentiated generalized Ramos-Louzada (EGRL) distribution

The EGRL distribution is a three-parameter generalization of the RL distribution, constructed by applying an exponentiation transformation to the CDF of the GRL distribution, which itself extends the base one-parameter RL via an additional shape parameter for greater tail flexibility [25]. The CDF of EGRL distribution is given as:

$$F_{\text{EGRL}}(z;\gamma,\eta,\kappa)=\left[1-\left(\frac{(\gamma+\gamma^{-1}z-1)e^{-\frac{z}{\gamma}}}{(\gamma-1)}\right)^{\eta}\right]^{\kappa},\ z>0,\eta>0,\kappa>0,\gamma\geq 2 \tag{7}$$

Then, the PDF of EGRL distribution is given as:

$$\begin{aligned} f_{\text{EGRL}}(z;\gamma,\eta,\kappa)=&\ \tfrac{\eta\kappa(\gamma+\gamma^{-1}z-1)e^{-\frac{z}{\gamma}}}{(\gamma-1)}\left[\tfrac{(\gamma+\gamma^{-1}z-1)e^{-\frac{z}{\gamma}}}{(\gamma-1)}\right]^{\eta-1}\times \\ &\left[1-\left(\tfrac{(\gamma+\gamma^{-1}z-1)e^{-\frac{z}{\gamma}}}{(\gamma-1)}\right)^{\eta}\right]^{\kappa-1},\ z>0,\eta>0,\kappa>0,\gamma\geq 2 \end{aligned} \tag{8}$$

6. Inverse Ramos-Louzada (IRL) distribution

In 2025, Hassan, Metwally [26] introduced an inverse transformation of form $w=1/z$ for the random variable that has RL distribution. The CDF and PDF for IRL distribution can be determined from the following equations:

$$F_{\text{IRL}}(w;\gamma)=\frac{(\gamma+1/\gamma w-1)e^{-1l\gamma w}}{(\gamma-1)},\quad w>0,\ \gamma\geq 2 \tag{9}$$

$$f_{\text{IRL}}(w;\gamma)=\frac{((\gamma-2)\gamma w+1)e^{-1l\gamma w}}{\gamma^2(\gamma-1)w^3},\quad w>0,\ \gamma\geq 2 \tag{10}$$

7. Ramos-Louzada exponential (RLE) distribution

Aljohani, Zaghdoun [27] in 2025 proposed another a two-parameter continuous lifetime model obtained by imposing RL logic on an exponential baseline distribution, giving it the advantage of a PDF and a CDF that have a more flexible skewed or complex data. It has a scale and shape parameter allowing monotone or non-monotone hazard rate to be used in environmental and reliability applications. A random variable $z$has a RLE distribution if its CDF and PDF are respectively given by

$$F_{\text{RLE}}(z;\gamma,\theta)=1-\left[1+\frac{\theta z}{\gamma(\gamma-1)}\right]e^{-\frac{\theta z}{\gamma}},\quad z>0,\ \gamma\geq 2,\ \theta>0 \tag{11}$$

and

$$f_{\text{RLE}}(z;\gamma,\theta)=\frac{\theta z(\gamma^2-2\gamma+\theta z)}{\gamma^2(\gamma-1)}e^{-\frac{\theta z}{\gamma}},\quad z>0,\ \gamma\geq 2,\ \theta>0 \tag{12}$$

8. Modeling evaluation

Different methods and strategies have been used to choose the right statistical distributions for wind speed. Measurement that gives the wind speed model that fits best based on data from the fitted model that was observed and predicted [16, 38, 39, 40, 41, 42]. The coefficient of determination (R^2), root mean square error (RMSE), Akaike information criterion (AIC), Bayesian information criterion (BIC), and Kolmogorov–Smirnov (KS) test are some of these.

The R^2 is calculated by Eq. (13) and is used to find the linear relationship between the observed probabilities and the predicted probabilities by a distribution.

$$\mathrm{R}^2 = \frac{\sum_{i=1}^{n}(\hat{G}_i - \bar{G})^2}{\sum_{i=1}^{n}(\hat{G}_i - \bar{G})^2 + \sum_{i=1}^{n}(G_i - \hat{G}_i)^2}, \tag{13}$$

where $\hat{G}_i$ is the predicted cumulative probabilities obtained from CDF, $G_i$is the observed cumulative probabilities, $\bar{G} = (1/n)\sum_{i=1}^{n}\hat{G}_i$.
The RMSE shows how accurate the model is by comparing the probabilities that were observed with the probabilities that were predicted. It is defined as

$$\mathrm{RMSE} = \sqrt{\left(\frac{1}{n}\sum_{i=1}^{n}(G_i - \hat{G}_i)^2\right)}. \tag{14}$$

AIC and BIC are defined

$$\mathrm{AIC} = -2\mathrm{log(L)} + 2\mathrm{p}. \tag{15}$$

$$\mathrm{BIC} = -2\log(L) + p\log n. \tag{16}$$

where $L$is the likelihood and $p$is the number of parameters in the models.

The KS test uses the empirical cumulative distribution function, which means it uses all of the data. In the KS test, a small statistic value means that the theoretical expressions fit the given samples well. If the calculated statistic is lower than the critical value, the hypothesis that the samples come from the reference distribution is accepted; if not, the hypothesis is rejected. The KS test statistic is calculated by finding the largest absolute difference between the theoretical CDF of a distribution, $\mathrm{CDF}_{\mathrm{Theorotical}}$, and the empirical CDF (ECDF). The KS test is shown by

$$\mathrm{D_{KS}} = \max_{1\le i\le n} \left|\mathrm{CDF} - \mathrm{ECDF}\right|, \tag{17}$$

where max is the largest distance between CDF and ECDF. If the wind speed data comes from the CDF distribution, then $\mathrm{D_{KS}}$ goes to 0. A higher value of R^2, a lower value of RMSE, AIC, and BIC all mean that the distribution function model works better.

9. Results and discussion

Maximum likelihood estimation (MLE) was used to fit each chosen PDF of the distribution to the wind speed series. Then, the evaluation criteria were calculated. Table 2 shows the minimum, maximum, mean, variance, coefficient of skewness, and coefficient of kurtosis for each location. The four locations range from 2.75 m/s to 4.76 m/s. The Basrah location has the fastest average wind speed of all the places we looked at, while the Al-Sulaymaniyah location has the slowest. The average wind speeds at Basrah and Al-Kut are very similar. The Basrah location has the most different wind speeds, followed by the Al-Kut location. The Al-Sulaymaniyah location has the most consistent wind speed because it has the least amount of change. The coefficient of skewness for all locations is positive, which means that all of the distributions used RL, GRL, IPRL, EGRL, IRL, and RLE are right-skewed. The coefficients of kurtosis, on the other hand, vary moderately, from -0.01 to 1.08.

Basrah (-0.07) and Al-Kut (-0.01) are slightly platykurtic, indicating flatter distributions with less pronounced peaks, whereas Tikrit (0.49) and especially Al-Sulaymaniyah (1.08) are positively kurtotic, indicating relatively more peaked distributions and greater tail concentration. These results show that although all sites share positive asymmetry, their distributional shapes differ in peakedness and tail behavior. The kurtosis values provide insight into the variability structure of wind speeds across the sites. Basrah (-0.07) and Al-Kut (-0.01) exhibit slightly negative excess kurtosis, indicating platykurtic distributions characterized by flatter shapes and more uniformly distributed wind speeds around the mean. This suggests relatively stable wind regimes with fewer pronounced

extreme events. In contrast, Al-Sulaymaniyah (1.08) shows positive kurtosis, indicating a more peaked (leptokurtic) distribution with heavier tails, implying greater intermittency and a higher likelihood of deviations from the mean wind speed. These differences likely reflect the influence of local terrain and atmospheric conditions, with more complex or variable flow regimes contributing to the higher kurtosis observed in Al-Sulaymaniyah.

Table 2. Statistical descriptive of the used locations

Location	N	Mean	Variance	Minimum	Maximum	Skewness	Kurtosis
Basrah	8091	4.7643	5.1936	0.0500	13.2600	0.57	-0.07
Al-Sulaymaniyah	8091	2.7457	2.1084	0.0200	10.3100	1.02	1.08
Tikrit	8091	3.6539	2.8391	0.0600	11.7700	0.63	0.49
Al-Kut	8091	4.3065	4.7310	0.0600	11.8600	0.60	-0.01

In order to compare the modeling performances of RL, GRL, IPRL, EGRL, IRL, and RLE distributions, the MLE estimate values of each distribution parameter are presented in Table 3.

Table 3. MLE parameter estimation of wind speed distributions

Distribution	Parameter	Locations			
		Basrah	Al-Sulaymaniyah	Tikrit	Al-Kut
RL	$\hat{\gamma}$	2.318	2.641	2.549	2.325
GRL	$\hat{\gamma}$	2.047	2.123	2.138	2.087
	$\hat{\beta}$	0.805	0.824	0.836	0.811
IPRL	$\hat{\gamma}$	2.212	2.241	2.235	2.228
	$\hat{\alpha}$	1.514	1.536	1.604	1.527
EGRL	$\hat{\gamma}$	2.147	2.361	2.384	2.207
	$\hat{\eta}$	0.571	0.664	0.629	0.592
	$\hat{\kappa}$	1.343	1.468	1.477	1.351
IRL	$\hat{\gamma}$	3.541	3.174	3.195	3.607
RLE	$\hat{\gamma}$	2.041	2.105	2.117	2.084
	$\hat{\theta}$	0.841	0.722	0.767	0.893

Table 4 shows the obtained evaluation criteria of all examined distributions, RL, GRL, IPRL, EGRL, IRL, and RLE, for Basrah, Al-Sulaymaniyah, Tikrit, and Al-Kut locations. The ranking of each distribution is presented in the last column of Table 4.

As shown in Table 4, the five criteria show that the IRL distribution is clearly better than all the other distributions in relation to the Basrah location results. The IRL distribution has the highest R^2 value and the lowest values for the RMSE, AIC, BIC, and KS. For instance, the IRL distribution had an RMSE of 0.0349, which is lower than the RMSEs of the RL, GRL, IPRL, EGRL, and RLE distributions. The IPRL and EGRL distributions also do better than the other distributions. The results also show that the RLE distribution cannot give a good estimate of the wind speed data that was measured at the Basrah station.

The IRL and IPRL distributions perform better than the other distributions at the Al-Sulaymaniyah location when measured by R^2, RMSE, AIC, BIC, and KS. When it comes to evaluation criteria, RL distribution is also better. The IRL distribution lowers RMSE by about 6.37%, 3.29%, 30.57%, 11.03%, and 18.12% compared to RL, IPRL, GRL, EGRL, and RLE, respectively. On the other hand, the GRL distribution doesn't seem to be good enough for modeling wind speed data for the Al-Sulaymaniyah location.

In the Tikrit location, IRL distribution comes out on top when using the R^2, RMSE, AIC, BIC, and KS criteria values. From Table 4, it is easy to see that the IPRL and RL distributions also do a good job of modeling wind speed data for this location. The RLE and EGRL distributions, on the other hand, are not good enough to model wind speed data for the Tikrit area.

Finally, for the Al-Kut location, IRL distribution has the best fits to the wind data because it has the highest R2 and the lowest RMSE, AIC, BIC, and KS values. IPRL distribution can also be the best second choice based on the R2, RMSE, AIC, BIC, and KS values. RLE distribution does not perform better than the other distributions.

The most important thing to learn from Table 4 is that the best fitting wind speed distributions are not the same in all places. The R^2, RMSE, AIC, BIC, and KS criteria caused big differences in the fitting results. In the Basrah, Al-Sulaymaniyah, Tikrit, and Al-Kut areas, the IRL and IPRL distributions are the most flexible when it comes to wind speed data and are the best at modeling. The fitting using IRL seems impressive because it has lower RMSE, AIC, BIC, and KS values and higher R^2 values. Also, the RLE distribution can't give good wind speed data fitting distribution in any location. Another finding shows that for the Al-Sulaymaniyah and the Tikrit locations, the RL distribution can generally be considered as effective wind speed data, fitting with the superiority of IRL distribution.

Beyond statistical goodness-of-fit, the IRL distribution admits a physically interpretable structure for Iraqi wind regimes. The IRL model is obtained via an inverse transformation of the Ramos–Louzada lifetime distribution and is characterized by an asymmetric, unimodal density with an upside-down-bathtub hazard rate, enabling it to represent data with frequent low–moderate values and a heavy right tail of extreme events. In wind applications, this behavior is consistent with long periods of background flow interrupted by episodic strong winds generated by synoptic systems, thermal contrasts, or orographic channeling. The single IRL parameter acts as a combined scale–tail index: larger values simultaneously increase the typical wind speed level and the probability of high-speed exceedances, whereas smaller values correspond to weaker regimes with lighter tails. This interpretation aligns with our parameter estimates. Basrah and Al-Kut, characterized by higher mean speeds and Shamal- or convection-driven strong events over open or coastal terrain, exhibit the largest IRL parameter values (3.541 and 3.607), indicating heavier right tails and more frequent strong winds. Tikrit and Al-Sulaymaniyah, by contrast, have lower IRL parameters (3.195 and 3.174), reflecting more moderate central speeds; yet the positive skewness and kurtosis at Al-Sulaymaniyah show that the IRL tail still captures terrain-induced enhancements during frontal passages in winter. Thus, the IRL distribution is not only a superior statistical fit but also provides a compact, physically meaningful descriptor of how large-scale circulation (e.g., Shamal winds), surface roughness, and topography jointly shape the wind speed regimes in the four Iraqi cities.

Table 4. Evaluation criteria values of wind speed used distributions for all locations

Location	Distribution	Criteria					Rank
		R^2	RMSE	AIC	BIC	DKS	
Basrah	RL	0.9817	0.0438	23890	23903	0.0101	5
	GRL	0.9831	0.0426	23826	23843	0.0086	4
	IPRL	0.9862	0.0363	23729	23751	0.0055	2
	EGRL	0.9847	0.0384	23784	23803	0.0068	3
	IRL	0.9877	0.0349	23682	23706	0.0044	1
	RLE	0.9691	0.0516	23942	23978	0.0126	6
Al-Sulaymaniyah							
	RL	0.9727	0.0439	23807	23852	0.0072	3
	GRL	0.9555	0.0592	24020	24079	0.0143	6
	IPRL	0.9742	0.0425	23760	23807	0.0061	2
	EGRL	0.9712	0.0462	23862	23904	0.0085	4
	IRL	0.9758	0.0411	23664	23783	0.0053	1
	RLE	0.9695	0.0502	23904	23944	0.0103	5
Tikrit							
	RL	0.9666	0.0462	23860	23939	0.0083	3
	GRL	0.9651	0.0481	23920	23988	0.0112	4
	IPRL	0.9681	0.0402	23813	23891	0.0074	2
	EGRL	0.9634	0.0523	23957	24028	0.0087	5
	IRL	0.9697	0.0432	23719	23867	0.0063	1
	RLE	0.9621	0.0535	24021	24088	0.0129	6
Al-Kut							
	RL	0.9753	0.0463	23948	23992	0.0114	5
	GRL	0.9783	0.0409	23847	23892	0.0085	3
	IPRL	0.9798	0.0388	23787	23843	0.0068	2
	EGRL	0.9766	0.0451	23884	23932	0.0072	4
	IRL	0.9813	0.0332	23740	23795	0.0057	1
	RLE	0.9626	0.0541	24002	24069	0.0144	6

Figures 2 – 5 show the histograms with the best-fitting distributions for all the places we looked at in our study. All the figures show that the wind speed data fitting matched the results in Table 4.

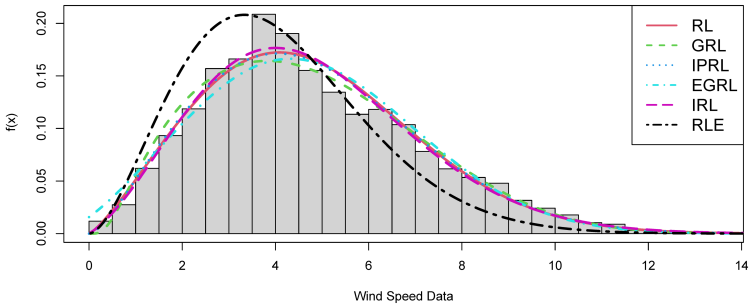

Figure 2. Distributions fitting of Basrah wind speed data location.

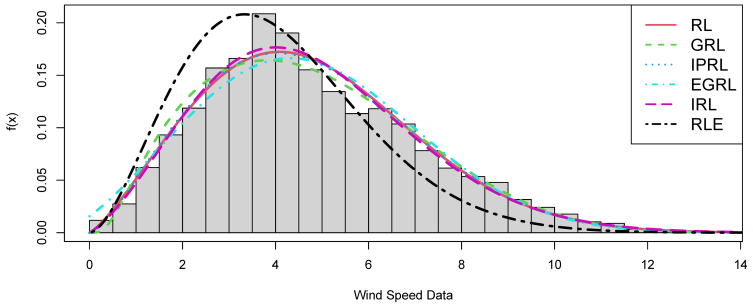

Figure 3. Distributions fitting of Al-Sulaymaniyah wind speed data location.

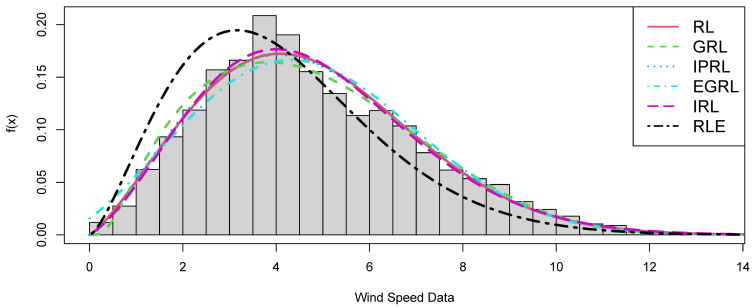

Figure 4. Distributions fitting of Tikrit wind speed data location.

To further illustrate the efficacy of the RL distribution and its extensions in modeling wind speed data, the optimal distribution at each location was compared with the Weibull distribution (WD), a widely employed distribution in wind speed data analysis. Table 5 gives a summary of the standards for judging the fitting distributions. According to the results in Table 5, IRL distribution fits the wind data better than WD for Basrah, Al-Sulaymaniyah, Tikrit, and Al-Kut. This is shown by the highest R^2 and the lowest RMSE, AIC, BIC, and KS values.

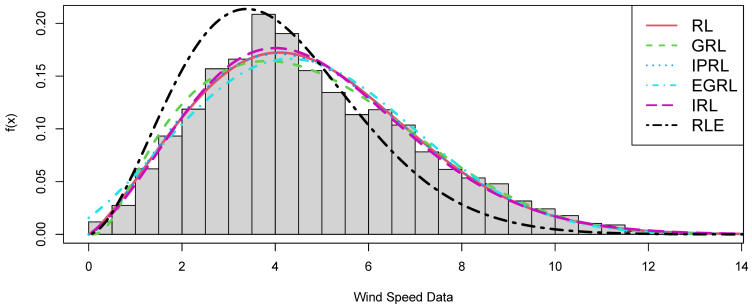

Figure 5. Distributions fitting of Al-Kut wind speed data location.

Table 5. Evaluation criteria values of wind speed used distributions for all locations

Location	Distribution	Criteria				
		R^2	RMSE	AIC	BIC	DKS
Basrah	WD	0.9609	0.0526	22918	22308	0.0092
	IRL	0.9877	0.0349	23682	23706	0.0044
Al-Sulaymaniyah						
	WD	0.9627	0.0651	22817	22903	0.0063
	IRL	0.9758	0.0411	23664	23783	0.0053
Tikrit						
	WD	0.9482	0.0617	22807	22955	0.0073
	IRL	0.9697	0.0432	23719	23867	0.0063
Al-Kut						
	WD	0.9569	0.0527	22919	22988	0.0083
	IRL	0.9813	0.0332	23740	23795	0.0057

10. Conclusion

The RL distribution and its extensions: GRL, IPRL, EGRL, IRL, and RLE provide superior modeling of hourly 2023 wind speed data from Iraqi cities Basrah, Al-Sulaymaniyah, Tikrit, and Al-Kut, all exhibiting positive skewness and moderate kurtosis. The MLE reveal IRL as the top performer across sites, with highest R^2 (0.9758–0.9877), lowest RMSE (0.0332–0.0432), AIC, BIC, and KS statistics, outperforming IPRL (second), RL, and RLE (consistently worst). Moreover, IRL also surpasses Weibull benchmarks by up to 52% in KS reduction. These distributions capture heavy-tailed, skewed wind regimes influenced by Iraq's geography, from Basrah's Shamal-driven highs to Al-Sulaymaniyah's terrain-moderated lows, advancing renewable energy assessments, turbine sizing, and environmental forecasting. As limitation, analysis relies on MERRA-2 reanalysis data at 10m height, potentially overlooking micro-scale turbulence or on-site measurement discrepancies. Future investigations could expand to multi-year MERRA-2 datasets or ground-based anemometer measurements from additional Iraqi governorates to assess temporal stability and spatial interpolation via geographically weighted regression. Hybrid models integrating RL extensions with machine learning (e.g., LSTM for time series or random forests for covariates like elevation and Shamal winds) may enhance predictive accuracy for wind farm viability.

REFERENCES

1. Akgül F. G. , Şenolu B. Arslan& T. *An alternative distribution to Weibull for modeling the wind speed data: Inverse Weibull distribution*, Energy Conversion and Management, vol. 114, pp. 234–240, 2016.
2. K. Bagci, T. Arslan, & H. E. Celik, *Inverted Kumarswamy distribution for modeling the wind speed data: Lake Van, Turkey*, Renewable and Sustainable Energy Reviews, vol. 135, 2021.
3. M. A. ul Haq, S. Hashmi, & M. Aslam, *Marshall-Olkin length biased exponential distribution for wind speed analysis alternative to Weibull distribution*, Modeling Earth Systems and Environment, vol. 10, no. 1, pp. 1095–1108, 2024.
4. T. Güney, *Renewable energy and sustainable development: Evidence from OECD countries*, Environmental Progress and Sustainable Energy, vol. 40, no. 4, 2021.

5. J. Jia, Z. Yan, X. Peng, & X. An, *A new distribution for modeling the wind speed data in Inner Mongolia of China*, Renewable Energy, vol. 162, pp. 1979–1991, 2020.
6. GLOBAL WIND ENERGY COUNCIL, *GLOBAL WIND REPORT 2024*, Available: www.gwec.net, 2024.
7. H. H. Gül, *Improved maximum likelihood estimators for the parameters of the two parameter lindley distribution*, Sigma Journal of Engineering and Natural Sciences, vol. 43, no. 1, pp. 290–300, 2025.
8. H. H. GUL & N. Yeniay Koçer, *Estimation of the Gompertz distribution's parameters under folded ranked set sampling*, Sigma: Journal of Engineering & Natural Sciences, vol. 43, no. 3, 2025.
9. A. A. Ahmed & Z. Y. Algamal, *Bias Reduction of Maximum Likelihood Estimation In Generalized Ramos-Louzada Distribution*, Iraqi Journal of Science, vol. 66, no. 7, pp. 2888–2901, 2025.
10. A. A. Ahmed, Z. Y. Algamal, & O. Albalawi, *Bias Reduction of Maximum Likelihood Estimation in the Inverse Xgamma Distribution*, Contemporary Mathematics, pp. 3174–3183, 2024.
11. A. A. Ahmed, Z. Y. Algamal, & O. Albalawi, *Bias reduction of maximum likelihood estimation in exponentiated Teissier distribution*, Frontiers in Applied Mathematics and Statistics, vol. 10, p. 1351651, 2024.
12. K. Mohammadi, O. Alavi, A. Mostafaeipour, N. Goudarzi, & M. Jalilvand, *Assessing different parameters estimation methods of Weibull distribution to compute wind power density*, Energy Conversion and Management, vol. 108, pp. 322–335, 2016.
13. M. Khalid Saeed, A. Salam, A. U. Rehman, & M. Abid Saeed, *Comparison of six different methods of Weibull distribution for wind power assessment: A case study for a site in the Northern region of Pakistan*, Sustainable Energy Technologies and Assessments, vol. 36, 2019.
14. J. Zhang, M. Zhang, Y. Li, J. Qin, K. Wei, & L. Song, *Analysis of wind characteristics and wind energy potential in complex mountainous region in southwest China*, Journal of Cleaner Production, vol. 274, 2020.
15. Y. M. Kantar, I. Usta, I. Arik, & I. Yenilmez, *Wind speed analysis using the Extended Generalized Lindley Distribution*, Renewable Energy, vol. 118, pp. 1024–1030, 2018.
16. O. Alavi, K. Mohammadi, & A. Mostafaeipour, *Evaluating the suitability of wind speed probability distribution models: A case of study of east and southeast parts of Iran*, Energy Conversion and Management, vol. 119, pp. 101–108, 2016.
17. Y. M. Kantar & I. Usta, *Analysis of the upper-truncated Weibull distribution for wind speed*, Energy Conversion and Management, vol. 96, pp. 81–88, 2015.
18. V. Lo Brano, A. Orioli, G. Ciulla, & S. Culotta, *Quality of wind speed fitting distributions for the urban area of Palermo, Italy*, Renewable Energy, vol. 36, no. 3, pp. 1026–1039, 2011.
19. K. Philippopoulos, D. Deligiorgi, & G. Karvounis, *Wind speed distribution modeling in the greater area of Chania, Greece*, International Journal of Green Energy, vol. 9, no. 2, pp. 174–193, 2012.
20. J. Y. Shin, T. B. M. J. Ouarda, & T. Lee, *Heterogeneous mixture distributions for modeling wind speed, application to the UAE*, Renewable Energy, vol. 91, pp. 40–52, 2016.
21. S. Chattopadhyay, T. Chakraborty, K. Ghosh, & A. K. Das, *Modified Lomax model: a heavy-tailed distribution for fitting large-scale real-world complex networks*, Social Network Analysis and Mining, vol. 11, no. 1, 2021.
22. L. A. Al-Essa, A. H. Abdel-Hamid, T. Alballa, & A. F. Hashem, *Reliability analysis of the triple modular redundancy system under step-partially accelerated life tests using Lomax distribution*, Scientific Reports, vol. 13, no. 1, 2023.
23. H. Al-Mofleh, A. Z. Afify, & N. A. Ibrahim, *A New Extended Two-Parameter Distribution: Properties, Estimation Methods, and Applications in Medicine and Geology*, Mathematics, vol. 8, no. 9, 2020.
24. A. Al Mutairi et al., *Inverse power Ramos–Louzada distribution with various classical estimation methods and modeling to engineering data*, AIP Advances, vol. 13, no. 9, 2023.
25. Y. AltİNİSİK & E. ÇAnkaya, *Exponentiated generalized Ramos-Louzada distribution with properties and applications*, Communications Faculty Of Science University of Ankara Series A1 Mathematics and Statistics, vol. 73, no. 1, pp. 76–103, 2023.
26. A. S. Hassan, D. S. Metwally, M. Elgarhy, & A. M. Gemeay, *A new probability continuous distribution with different estimation methods and application*, Computational Journal of Mathematical and Statistical Sciences, vol. 0, no. 0, pp. 0–0, 2025.
27. H. M. Aljohani et al., *A novel extension of the exponential distribution with application in modeling complex lifetime and environmental data*, Scientific Reports, vol. 15, no. 1, p. 33581, 2025.
28. J. K. Okutu, N. K. Frempong, A. O. Adebanji, & S. K. Appiah, *Modified Ramos-Louzada-G family with baseline Weibull distribution: Properties, characterizations, regression, and applications*, Scientific African, vol. 26, 2024.
29. F. Younis, M. Aslam, & M. I. Bhatti, *Preference of Prior for Two-Component Mixture of Lomax Distribution*, Journal of Statistical Theory and Applications, vol. 20, no. 2, pp. 407–424, 2021.
30. M. A. ul Haq, G. S. Rao, M. Albassam, & M. Aslam, *Marshall–Olkin Power Lomax distribution for modeling of wind speed data*, Energy Reports, vol. 6, pp. 1118–1123, 2020.
31. S. Jahan, N. Masseran, & W. Zin, *Wind speed analysis using Weibull and lower upper truncated Weibull distribution in Bangladesh*, Energy Reports, vol. 11, pp. 5456–5465, 2024.
32. P. Lencastre, A. Yazidi, & P. G. Lind, *Modeling Wind-Speed Statistics beyond the Weibull Distribution*, Energies, vol. 17, no. 11, 2024.
33. C. S. Rajitha & K. Anisha, *The odd Weibull Lindley distribution for modeling wind energy data*, International Journal of Data Science and Analytics, 2024.
34. A. N. Alkhateeb, & Q. N. N. Al-Qazaz, *Variable Selection in Weibull Accelerated Survival Model Based on Chaotic Sand Cat Swarm Algorithm*, Statistics, Optimization & Information Computing, vol. 13, no. 5, pp. 2105–2118, 2025.
35. J. K. Okutu, N. K. Frempong, S. K. Appiah, & A. O. Adebanji, *The Odd Ramos-Louzada Generator of distributions with applications to failure and waiting times*, Scientific African, vol. 22, 2023.
36. P. L. Ramos & F. Louzada, *A Distribution for Instantaneous Failures*, Stats, vol. 2, no. 2, pp. 247–258, 2019.
37. A. A. Ahmed & Z. Y. Algamal, *Bias Reduction of Maximum Likelihood Estimation In Generalized Ramos-Louzada Distribution*, Iraqi Journal of Science, pp. 2888–2901, 2025.
38. A. A. Ogunde, V. Eshomomoh Laoye, O. N. Ezichi, & K. O. Balogun, *Harris Extended Power Lomax Distribution: Properties, Inference and Applications*, International Journal of Statistics and Probability, vol. 10, no. 4, 2021.

39. F. G. Akgül & B. Şenoğlu, *Comparison of wind speed distributions: a case study for Aegean coast of Turkey*, Energy Sources, Part A: Recovery, Utilization, and Environmental Effects, vol. 45, no. 1, pp. 2453–2470, 2023.
40. N. Masseran, *Integrated approach for the determination of an accurate wind-speed distribution model*, Energy Conversion & Management, vol. 173, pp. 56–64, 2018.
41. S. M. Aljeddani & M. A. Mohammed, *An extensive mathematical approach for wind speed evaluation using inverse Weibull distribution*, Alexandria Engineering Journal, vol. 76, pp. 775–786, 2023.
42. M. M. Al-hashimi, & A. N. Alkhateeb, *Spatial analysis of brain and other cns cancers incidence in Iraq during 2000-2015*, Malaysian Journal of Public Health Medicine, vol. 20, no. 3, pp. 27–34, 2020.
43. T. B. M. J. Ouarda, C. Charron, & F. Chebana, *Review of criteria for the selection of probability distributions for wind speed data and introduction of the moment and L-moment ratio diagram methods, with a case study*, Energy Conversion and Management, vol. 124, pp. 247–265, 2016.
44. F. Al-Mutar & Z. Algamal, *Survival Function Estimation based on Neutrosophic two-parameter XLindley distribution* Statistics, Optimization & Information Computing, vol.14, no.3, pp. 1088–1097, 2025.
45. F. Al-Mutar & Z. Algamal, *Neutrosophic Exponentiated Power Lomax Distribution* Electronic Journal of Applied Statistical Analysis, vol.18, no.1, pp. 83–101, 2025.
46. N. M. Hammood, N. K. Rashad & Z. Y. Algamal *Neutrosophic Topp-Leone Extended Exponential distribution modeling with application for bladder cancer patients* International Journal of Neutrosophic Science, vol. 25, no. 1, pp.239-245, 2025.
47. O. E. Al-Saqal, Z. A. Hadied & Z. Y. Algamal *Modeling bladder cancer survival function based on neutrosophic inverse Gompertz distribution* International Journal of Neutrosophic Science, vol. 25, no. 1, pp.75-80, 2025.
48. M. Y. Mustafa & Z. Y. Algamal *Neutrosophic inverse power Lindley distribution: A modeling and application for bladder cancer patients* International Journal of Neutrosophic Science, vol. 21, no. 2, pp.216-223, 2023.
49. M. M. Alanaz, M. Y. Mustafa & Z. Y. Algamal *Neutrosophic Lindley distribution with application for Alloying Metal Melting Point* International Journal of Neutrosophic Science, vol. 21, no. 4, pp.65-71, 2023.
50. M. M. Alanaz & Z. Y. Algamal *Neutrosophic exponentiated inverse Rayleigh distribution: Properties and Applications* International Journal of Neutrosophic Science, vol. 21, no. 4, pp.36-42, 2023.
51. A. A. Bibani & Z. Y. Algamal *Survival Function Estimation for Fuzzy Gompertz Distribution with neutrosophic data* International Journal of Neutrosophic Science, vol. 21, no. 3, pp.137-142, 2023.
52. Algamal, Z., & Ali, H. M. *An efficient gene selection method for high-dimensional microarray data based on sparse logistic regression* , Electronic Journal of Applied Statistical Analysis, vol . 10 , no . 1 , 242-256 , 2017.
53. Naziyah, A. A., & Algamal, Z. Y. *Jackknifed Liu-type estimator in Poisson regression model* Journal of the Iranian Statistical Society, vol.19, no.1, p. 21-37, 2020.
54. Lukman, A. F., Dawoud, I., Kibria, B. G., Algamal, Z. Y., & Aladeitan, B. *A new ridge-type estimator for the gamma regression model* Scientifica, vol. 1, p.5545356, 2021.